Frequency of Debris Disks at White Dwarfs

Sara D. Barber

The University of Oklahoma
Homer L. Dodge Department of Physics and Astronomy

April 9, 2012

Detection Sensitivity

- Current detection techniques insensitive for $M_\star > 3M_\odot$

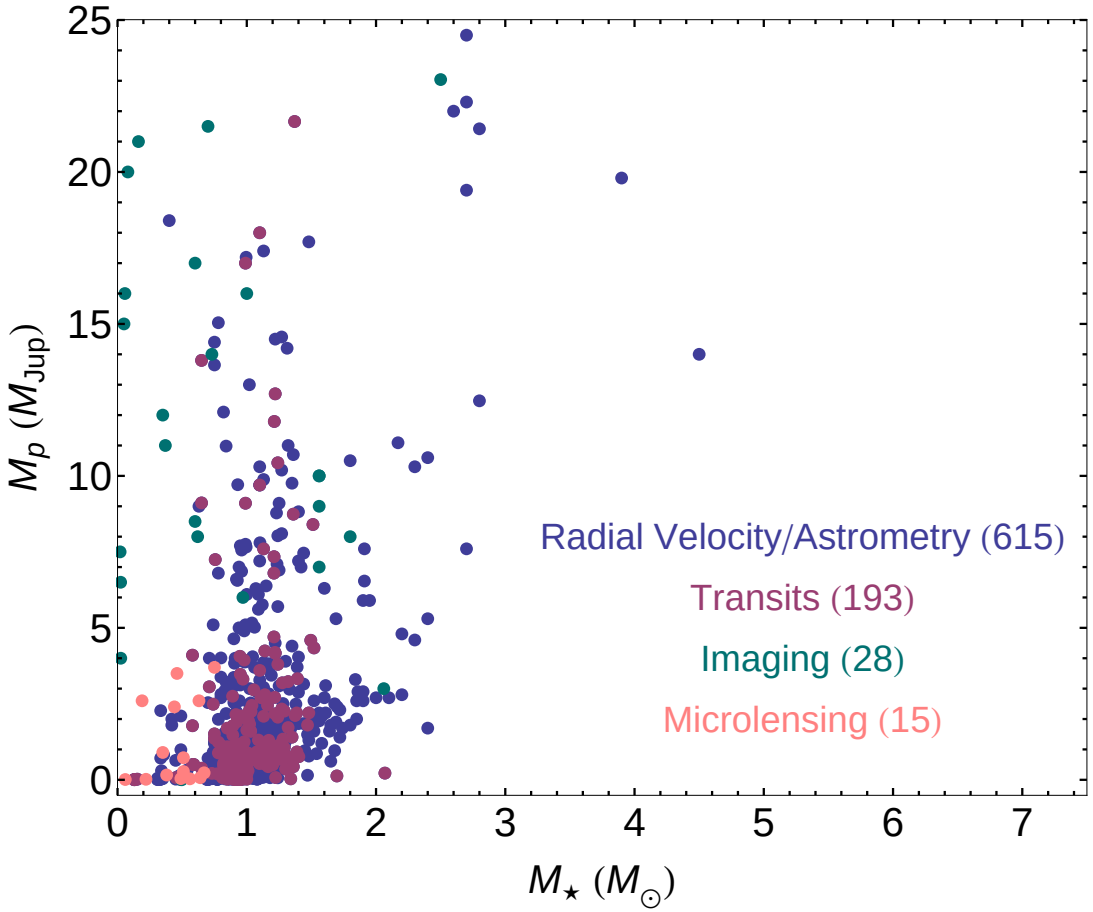

Figure: Data from The Extrasolar Planets Encyclopedia Catalog

Radial Velocity

- Massive stars
  - harder to move
  - fewer narrow absorption lines

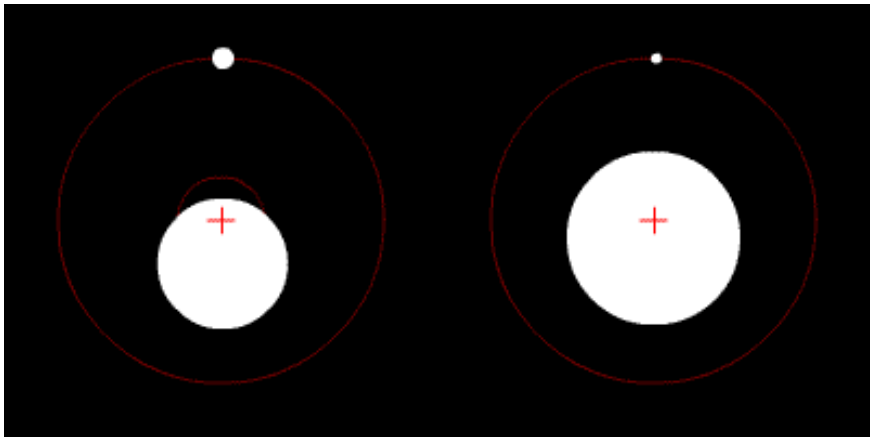

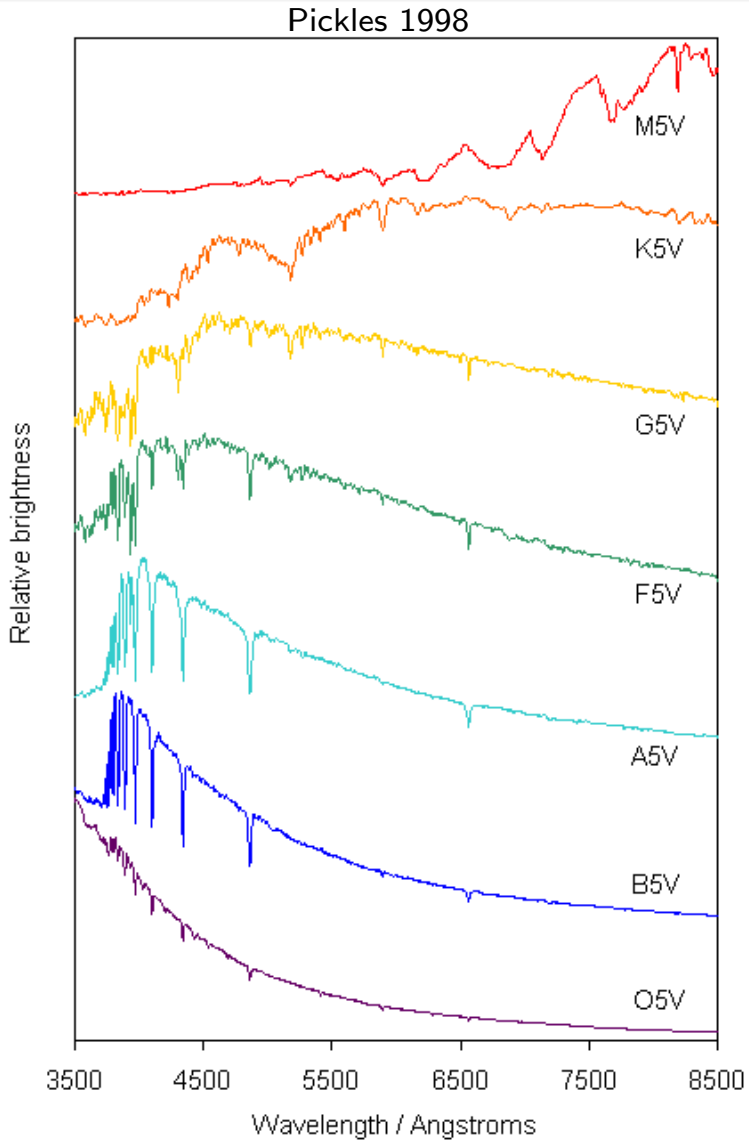

Transits

- Subtle dimming for massive stars

Pearson Education, Inc.

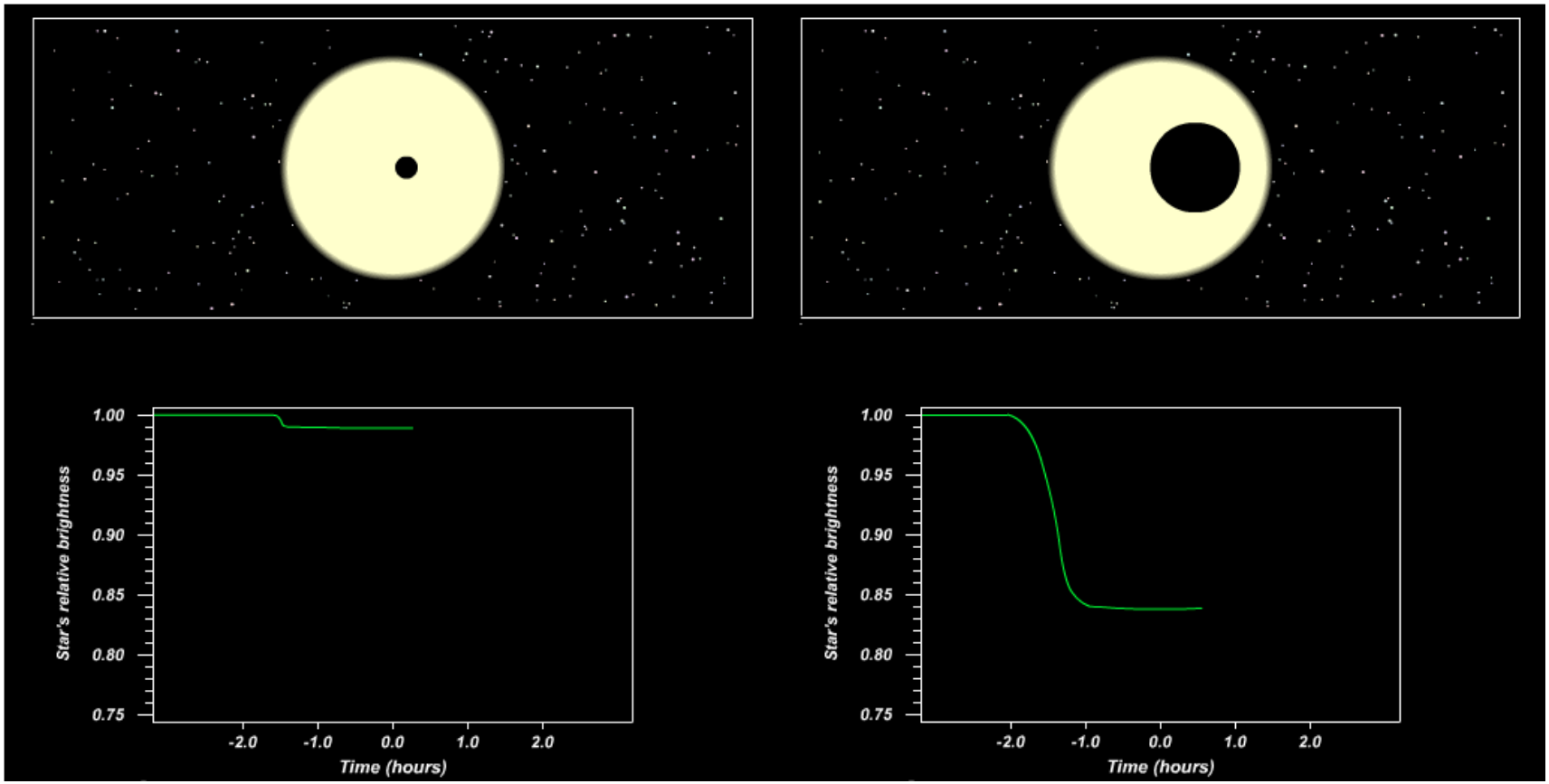

Imaging

- Reflected starlight / IR emission
- Massive star outshines planet

Max Planck Institute

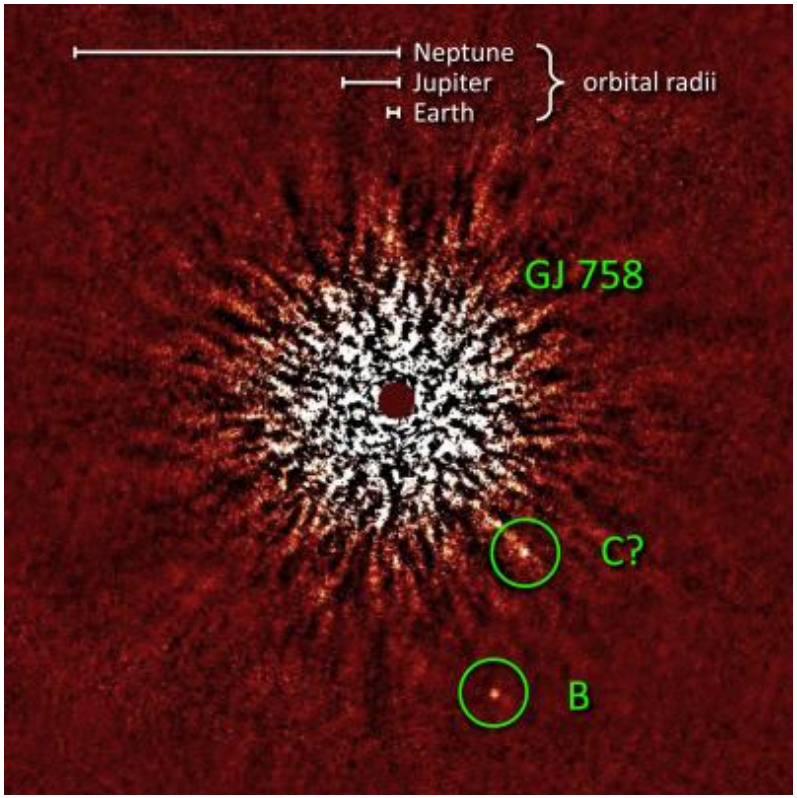

Figure: Near IR image taken of $10 - 40\ M_{jup}$ companion of sun-like star

Microlensing

- Planet signal washed out by massive star signal

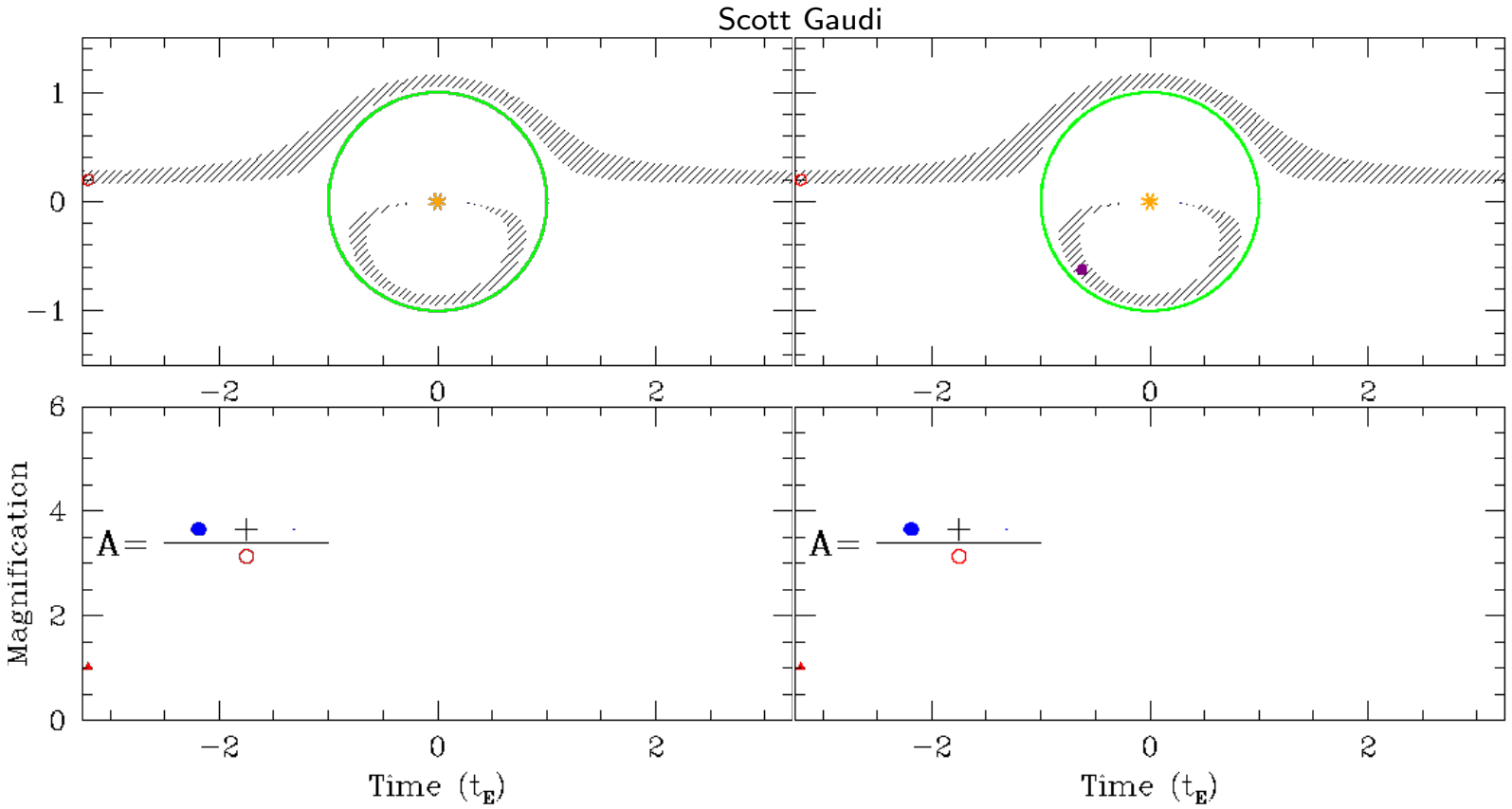

Microlensing

- Planet signal washed out by massive star signal ($q = m_p/m_\star$)

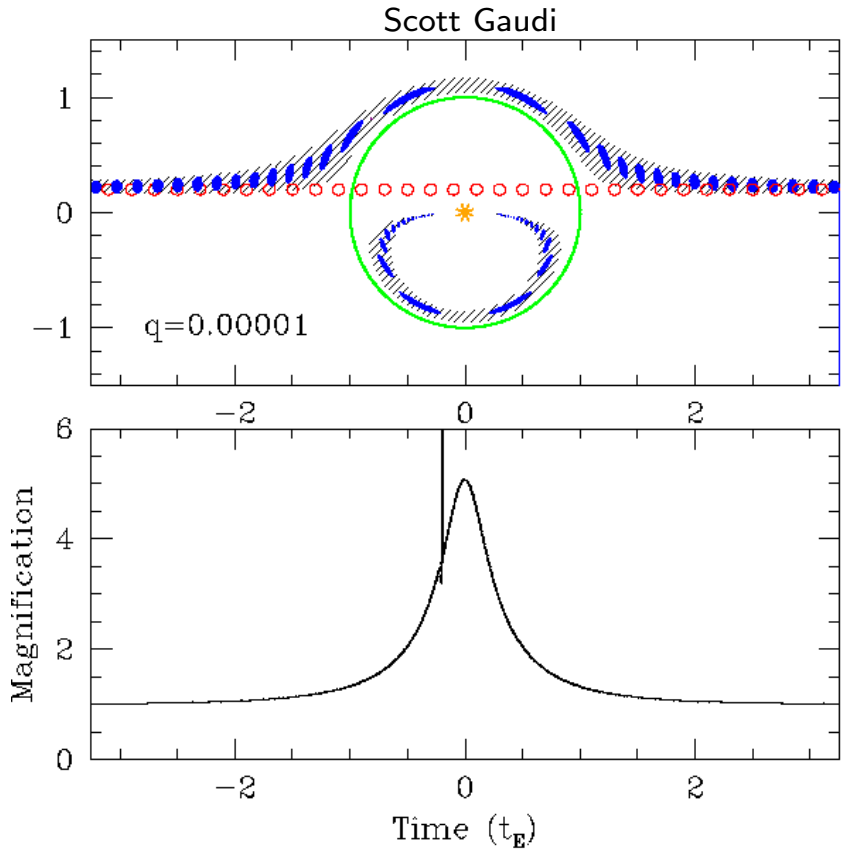

Indirect Probe

- Probe elusive regime using WD remnants
- Planetary systems destabilize
  - Giant planet resonances perturb planetesimals
  - Tidal disruption creates observable debris disk

NASA

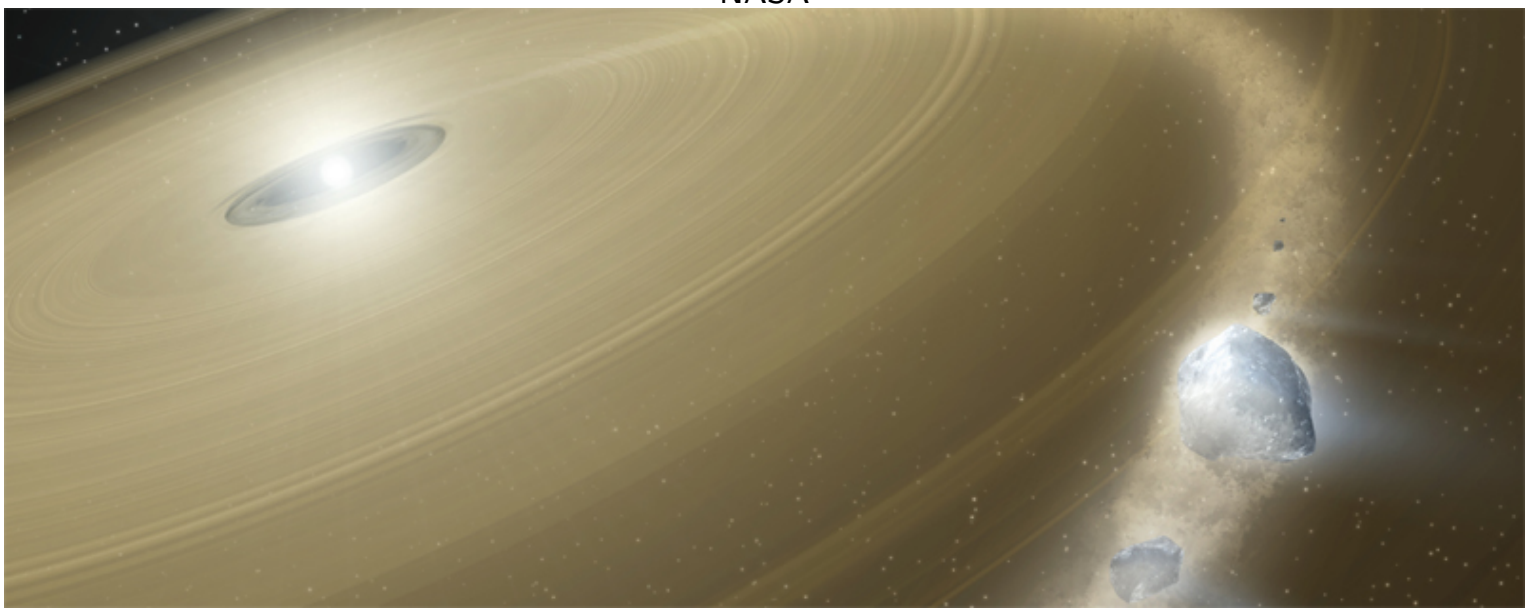

Figure: Debris disk around white dwarf

Indirect Probe

- SED – superposition of two blackbodies
- Peak location and intensity determined by disk geometry

NASA/JPL—Caltech

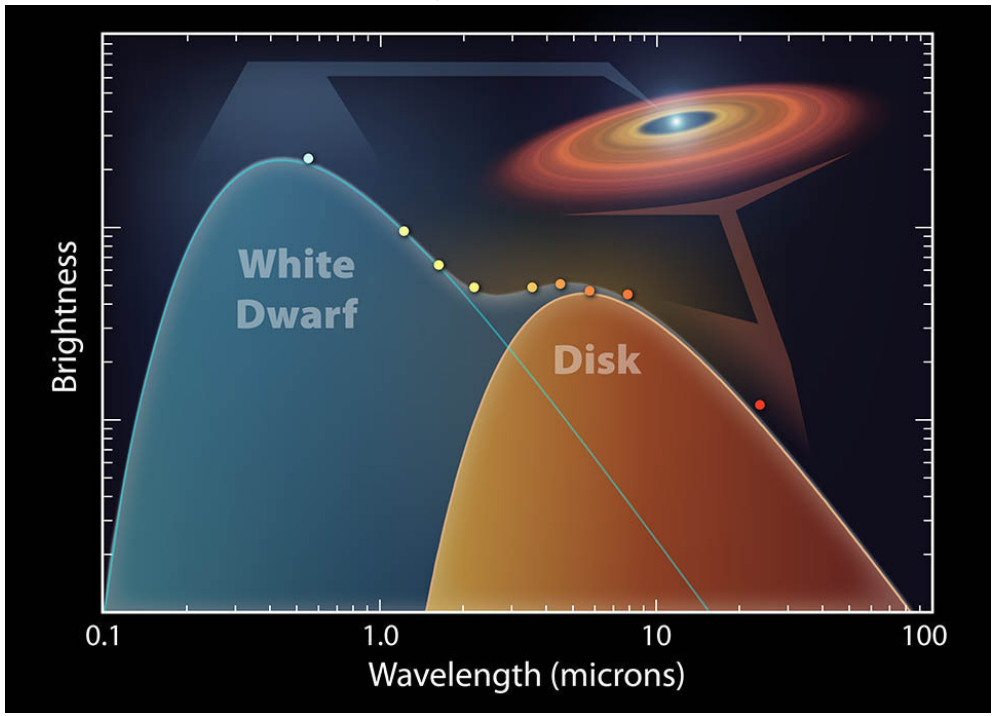

Figure: SED of a white dwarf + disk system GD 16

Indirect Probe

- Disk composition dominated by silicates

Reach et al. 2005

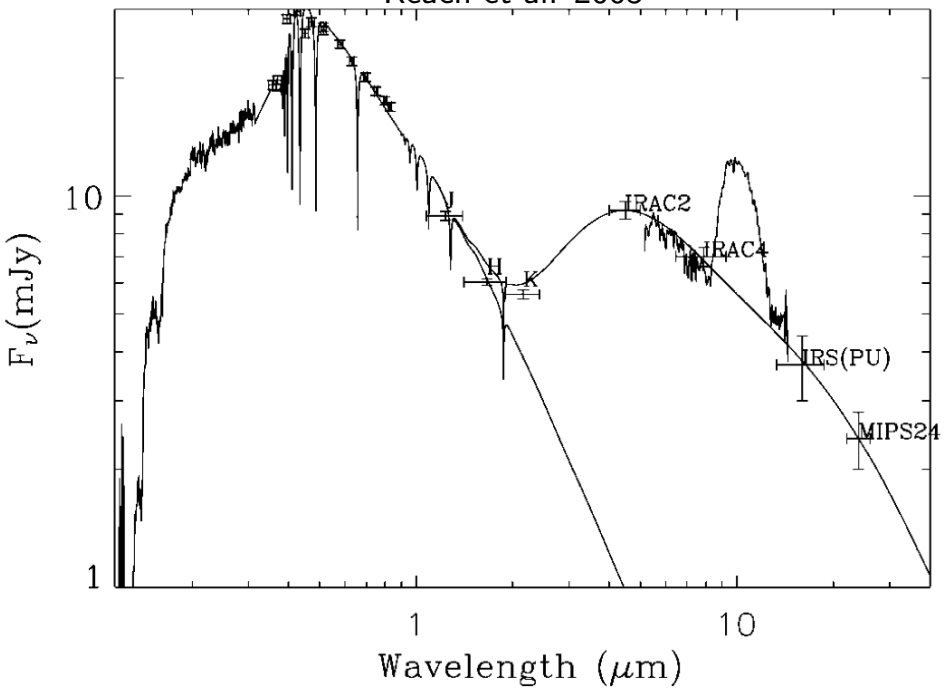

Figure: SED of PG2326+049

Reach et al. 2005

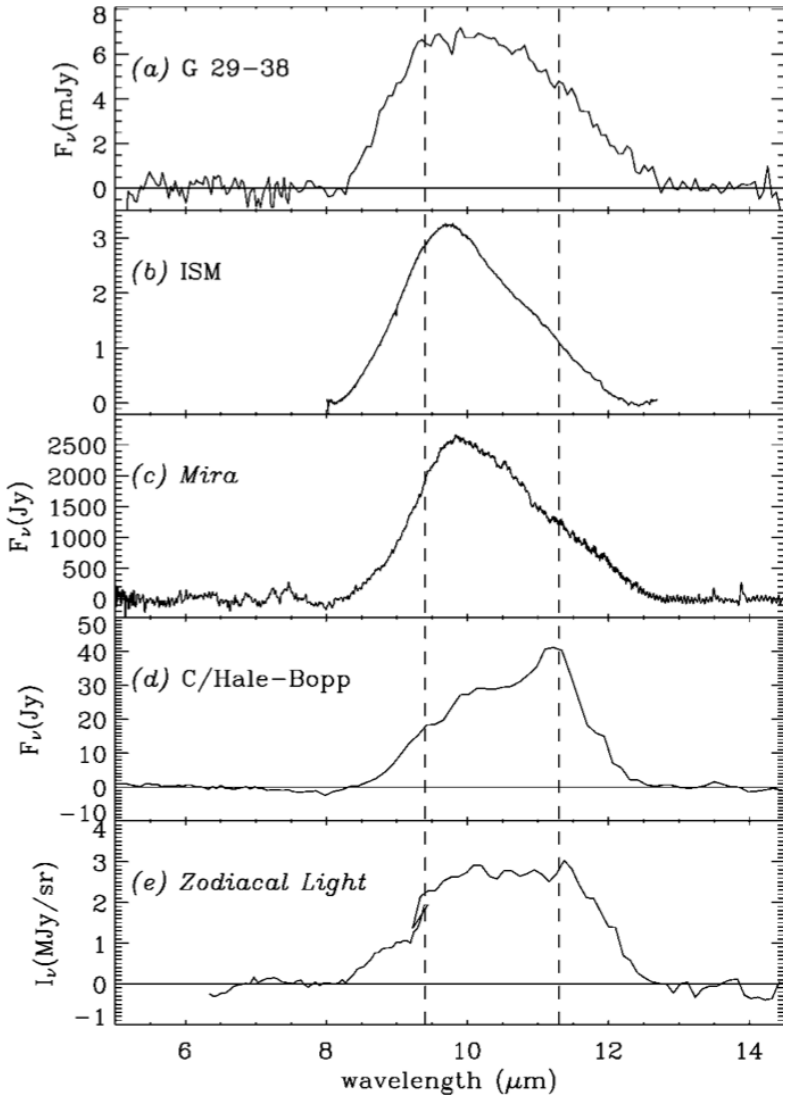

Indirect Probe

- Abundances similar to Solar System terrestrial bodies

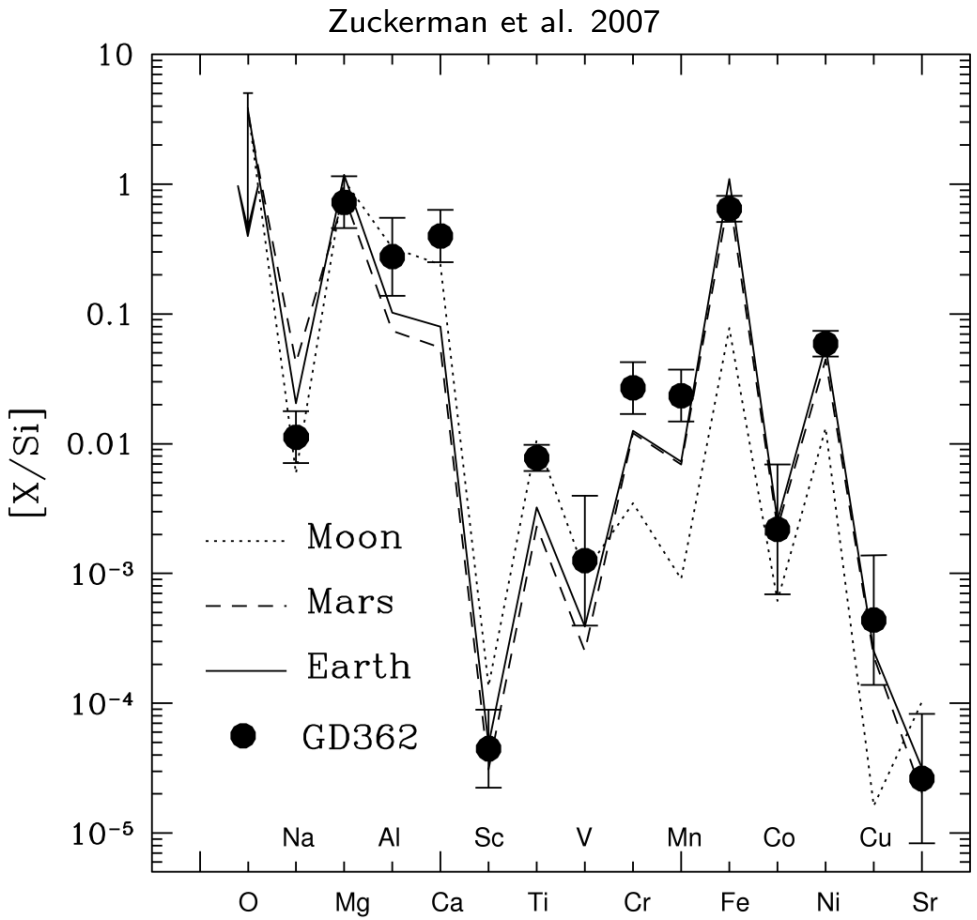

Figure: Elemental abundances by number relative to Silicon.

Indirect Probe

- Debris disks are tracers for planetary systems that have survived the death of their host star

Gemini Observatory — Jon Lomberg

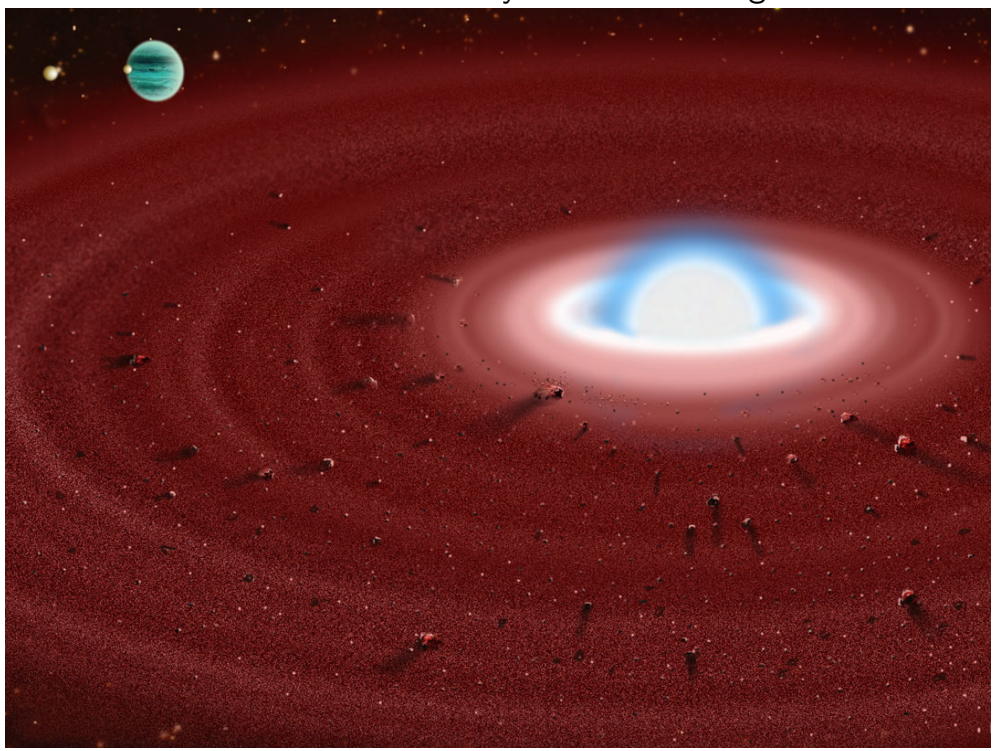

Figure: Visualization of dust disk around white dwarf GD 362 featuring hypothetical shepherding giant planet.

Resonances in the Solar System

- Numerical relation between periods
  - Spin-orbit coupling
  - Orbit-orbit coupling

Figure: Lunar synchronous rotation + small librations in latitude and longitude

Resonances in the Solar System

- Numerical relation between periods
  - Spin-orbit coupling
  - Orbit-orbit coupling

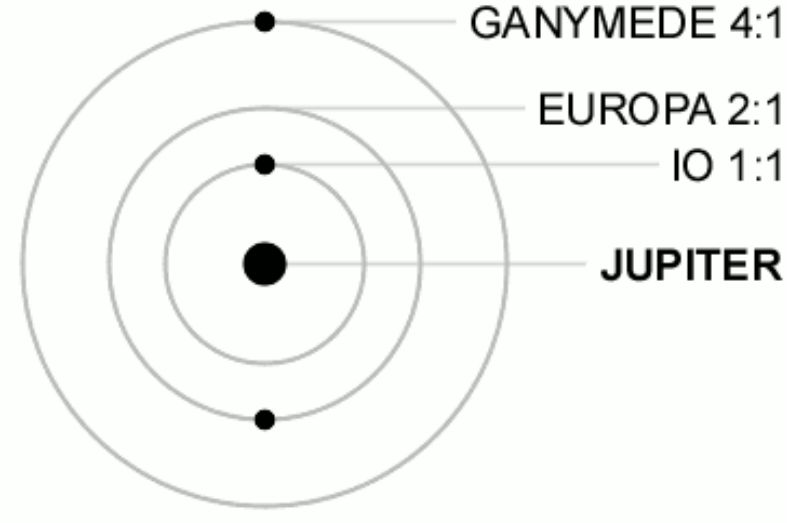

Figure: Mean motion resonance exhibited by three of the Galilean moons.

Resonances in the Solar System

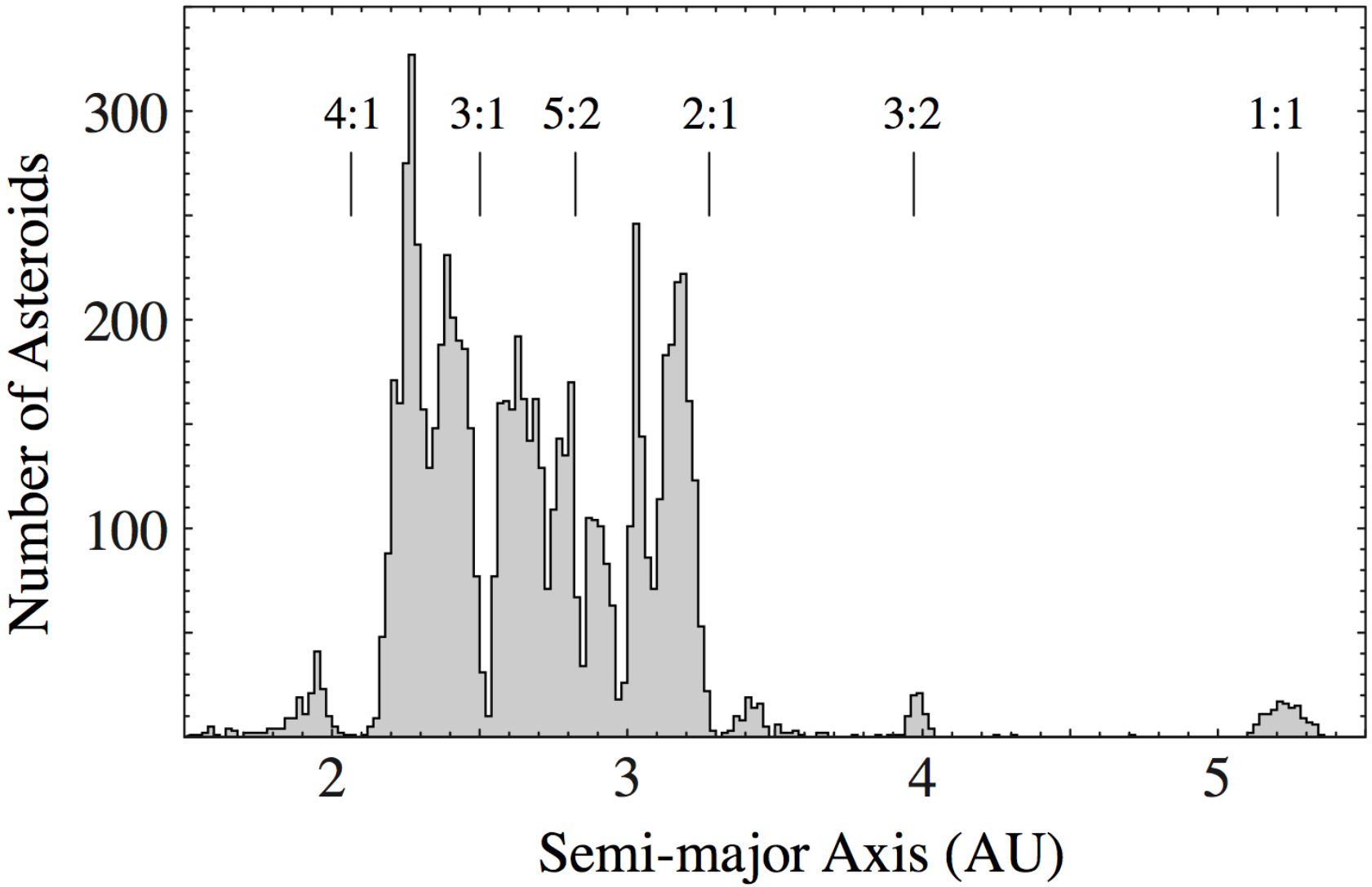

Post Main-Sequence Evolution

- Resonances more efficient at perturbing planetesimals during post main-sequence
- Mean motion resonances have finite width

$$\frac{\delta a_{\max}}{a} = \pm \left(\frac{16}{3} \frac{|C_r|}{n} e \right)^{1/2} \left(1 + \frac{1}{27 j_2^2 e^3} \frac{|C_r|}{n} \right)^{1/2} - \frac{2}{9 j_2 e} \frac{|C_r|}{n}$$

where

$$\frac{|C_r|}{n} = \frac{m_p}{m_\star} \alpha f_d(\alpha)$$

n – mean motion	e – asteroid eccentricity
a – asteroid semi-major axis	α – ratio asteroid/planet semi-major axes

Solar System Dynamics – Murray & Dermott (1999)

Post Main-Sequence Evolution

- AGB – star loses most of its mass
- Resonance widths increase
  - Asteroids previously exterior to resonance become trapped

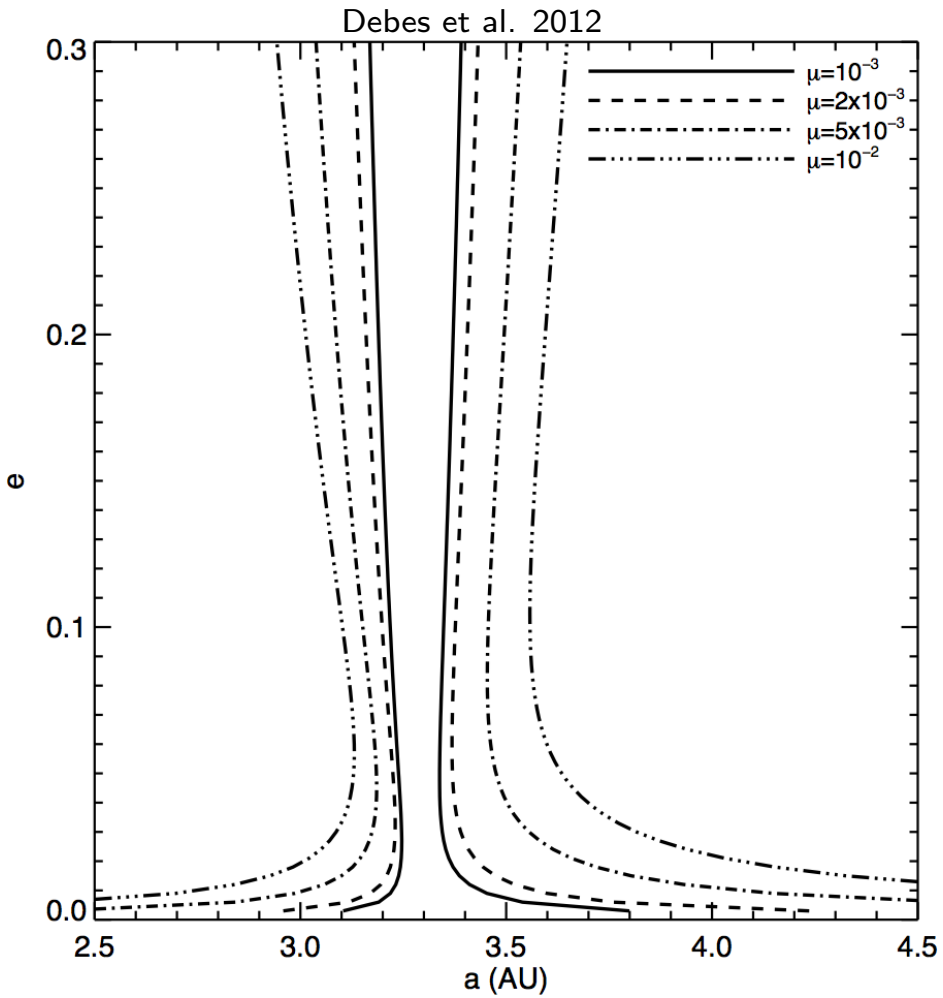

Figure: Growth of δa_{max} with increase of $\mu = m_p/m_\star$

Planetesimal Disruption

- Newly perturbed asteroids enter highly eccentric orbits
- Approach stellar remnant – tidally ripped apart

$$R_{tide} = C_{tide} R_{WD} \left(\frac{\rho_{WD}}{\rho_{ast}} \right)^{1/3}$$

- For $\left.\begin{array}{l} R_{WD} = 0.01\ R_{\odot} \\ M_{WD} = 0.69\ M_{\odot} \\ \rho_{ast} = 3\ \mathrm{g\ cm^{-3}} \end{array}\right\} R_{tide} = 0.7\ R_{\odot}$

NASA

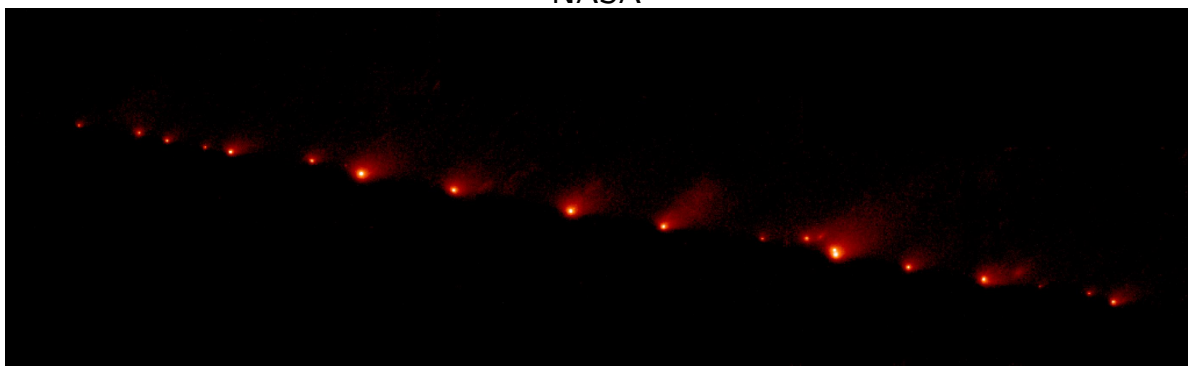

Figure: Fragmented Comet Shoemaker-Levy 9

Disk Formation

- Initially fragments stay on orbits similar to host
- Inward migration facilitated by Poynting-Robertson drag

$$\tan\left(\frac{\theta'}{2}\right) = \sqrt{\frac{c-v}{c+v}}\tan\left(\frac{\theta}{2}\right)$$

- Decay time $\sim .003 - 3$ Myr

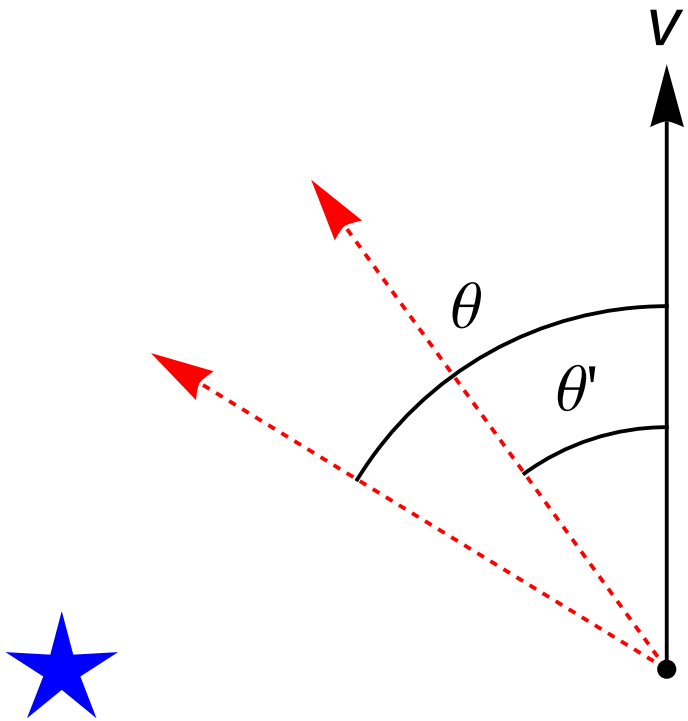

Figure: Relativistic aberration of light

Disk Formation

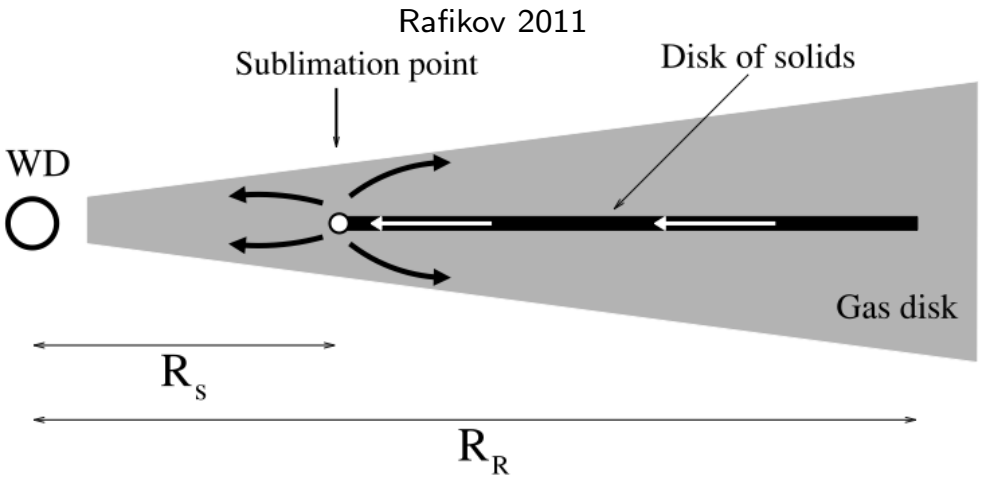

- Inner boundary set by sublimation radius (typically $\sim 0.1\ R_\odot$)
- Outer boundary set by radius of tidal disruption (typically $\sim 1\ R_\odot$)

Gemini Observatory — Jon Lomberg

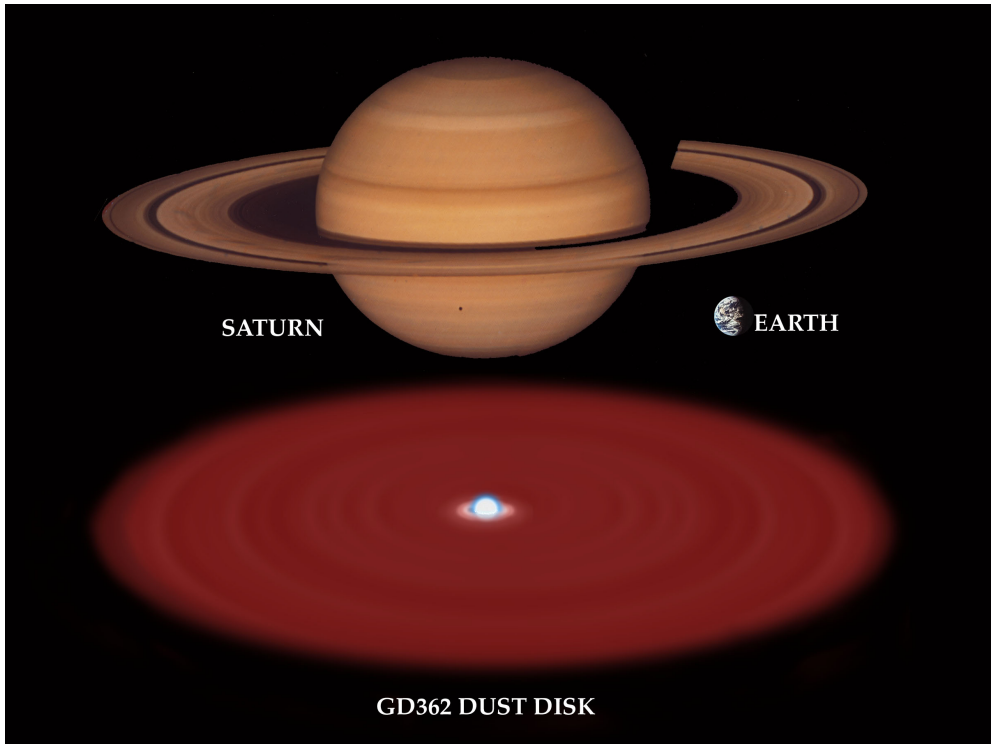

Figure: Debris disk surrounding white dwarf GD362

Sample

- 119 cool DA WDs from Palomar-Green catalogue

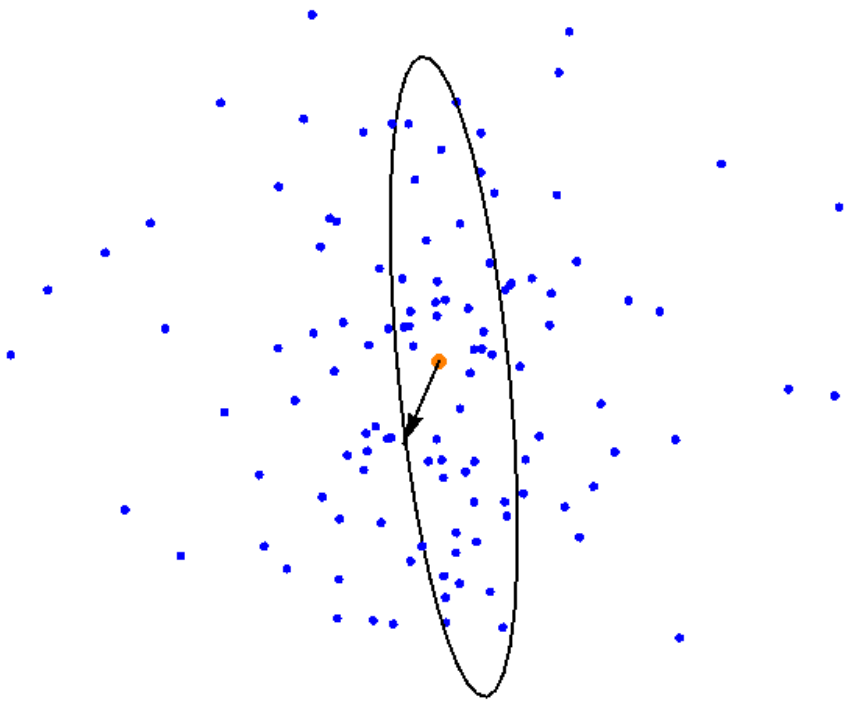

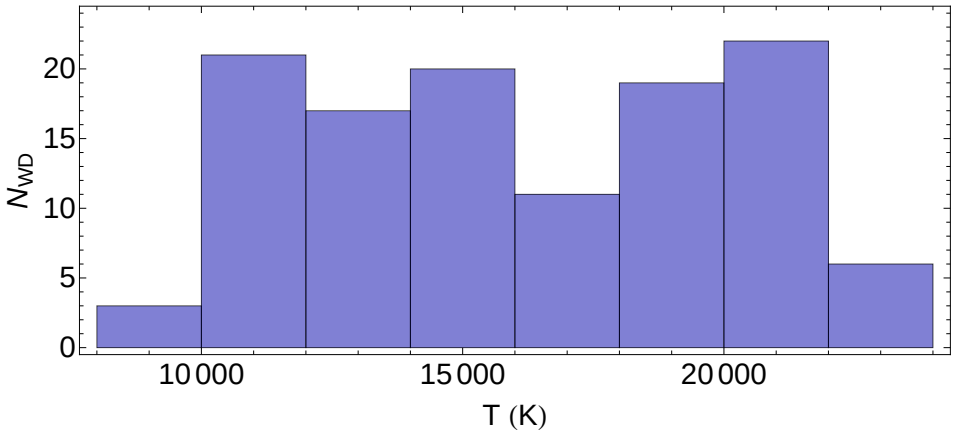

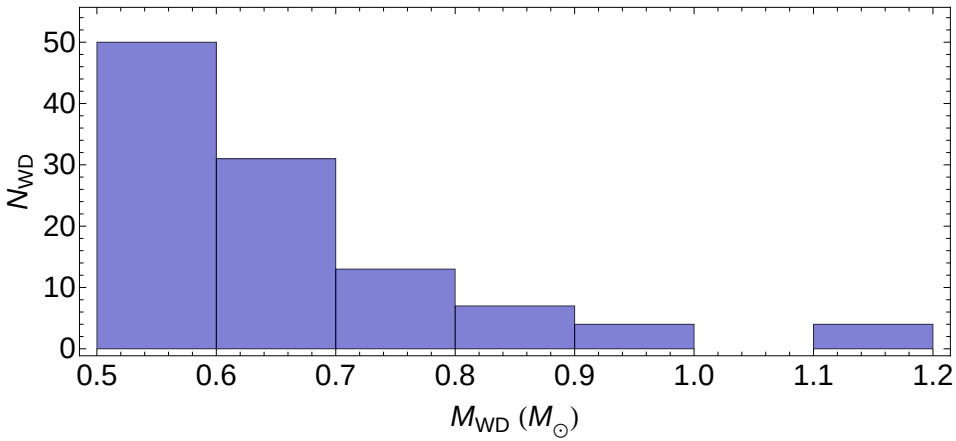

Photometry

- 114 WDs
- J (1.2μm), H (1.6μm), K (2.2μm)

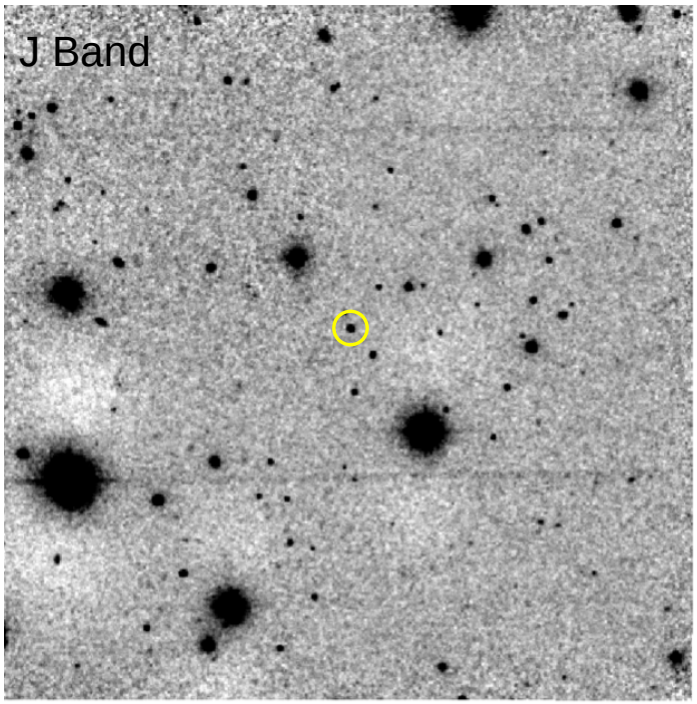

John McAfee

Figure: 1.3 m Peters Automated InfraRed Imaging TELescope (PAIRITEL)

Photometry

- 25 WDs
- 3.6, 4.5, 5.8, and 8 μm

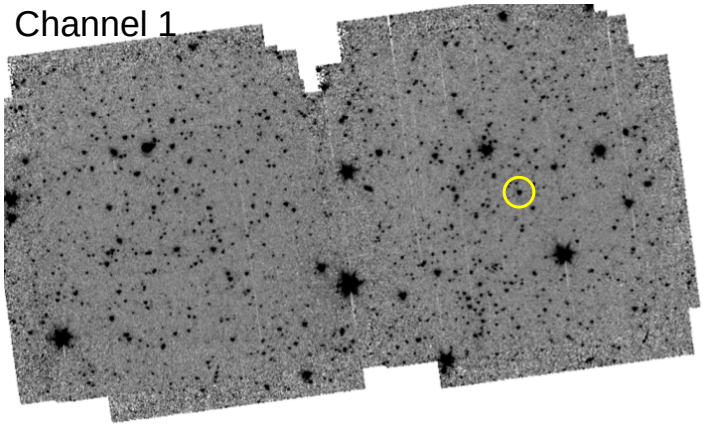

NASA/JPL—Caltech

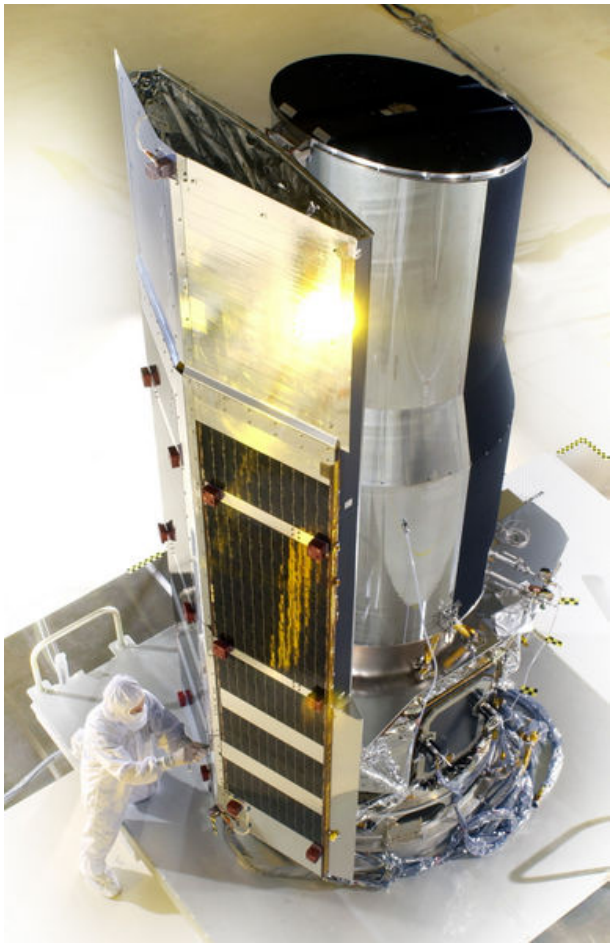

Figure: 0.85 m Spitzer Space Telescope prior to 2003 launch

Spectroscopy

- 42 WDs
- $0.8 - 5.4\mu$m
- $\frac{\lambda}{\Delta\lambda} = 150$

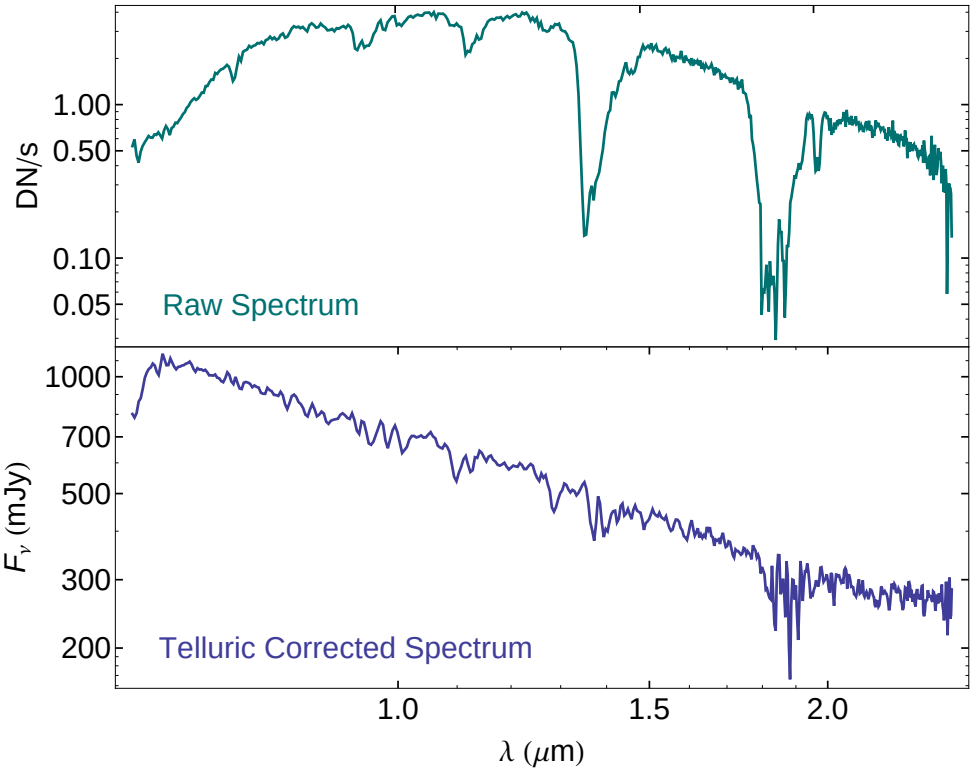

Henrik Melin

Figure: 3 m NASA InfraRed Telescope Facility (IRTF)

Blackbody Deviations

- Scale each WD's spectrum and blackbody to J-band photometry
- Look for excess $\geq 3\sigma$ deviation from blackbody

NASA/JPL—Caltech

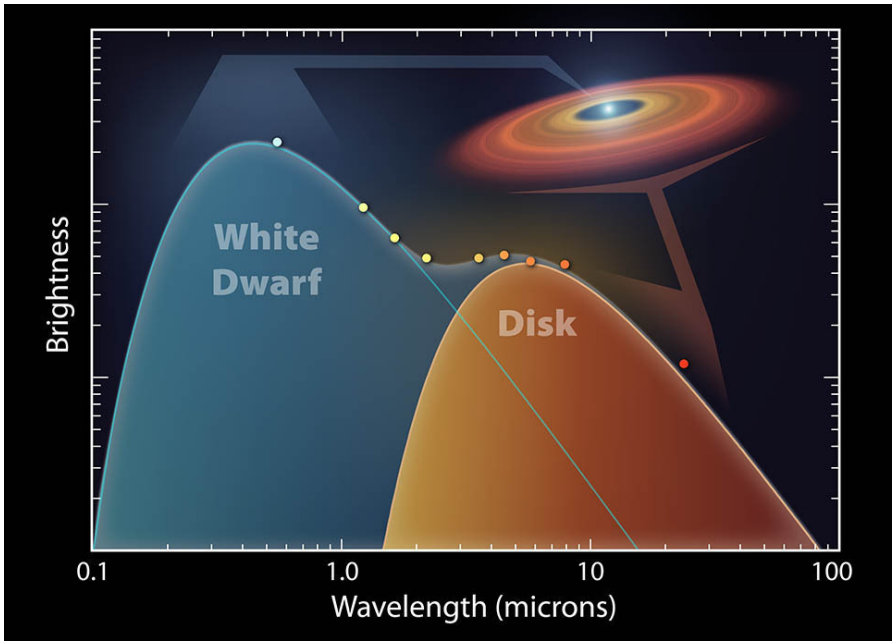

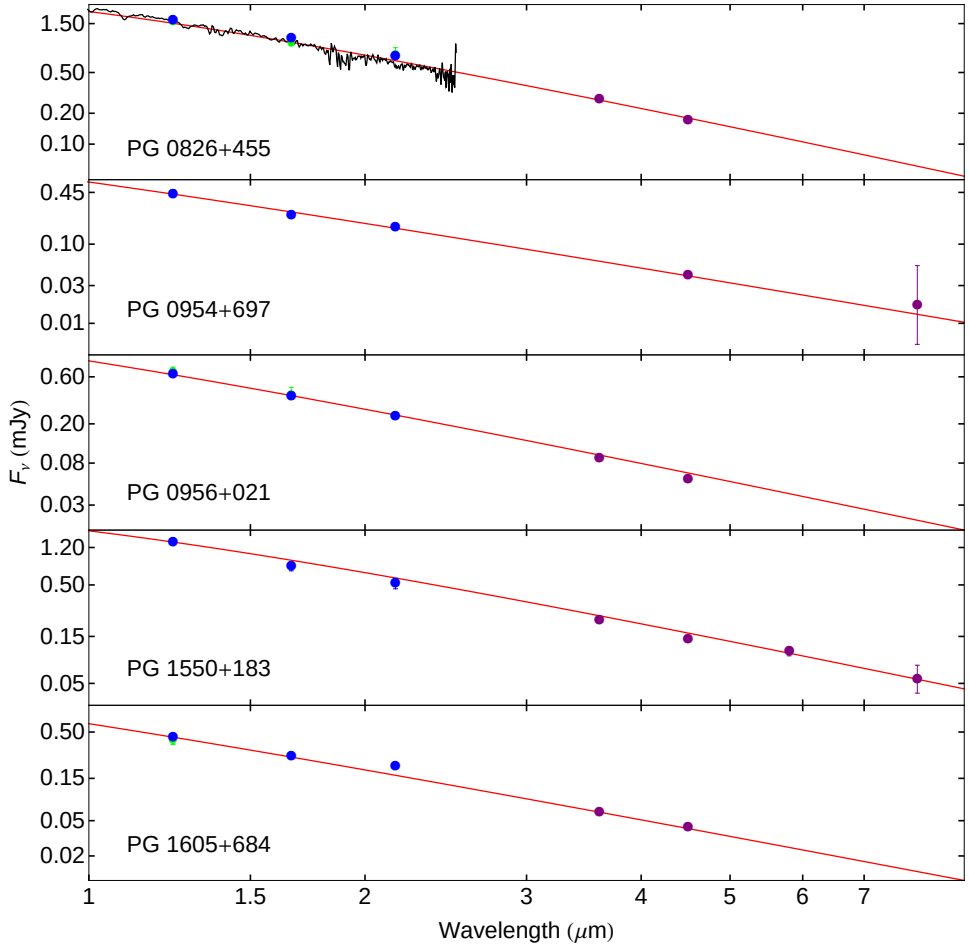

Figure: Five white dwarfs with non-detections of excess IR radiation

Blackbody Deviations

- 5 out of 119 white dwarfs exhibit excess IR emission
  - Frequency $= 4.2^{+2.7}_{-1.2}\%$

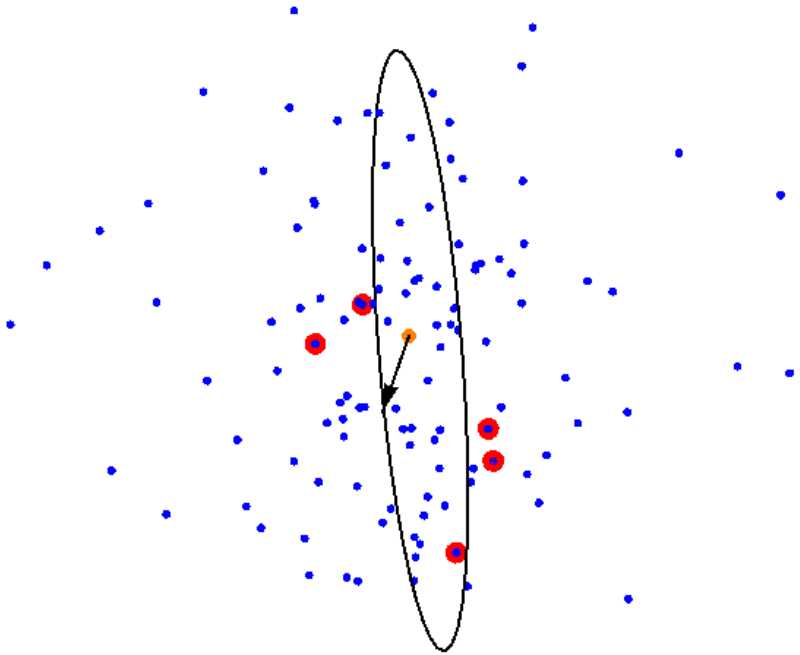

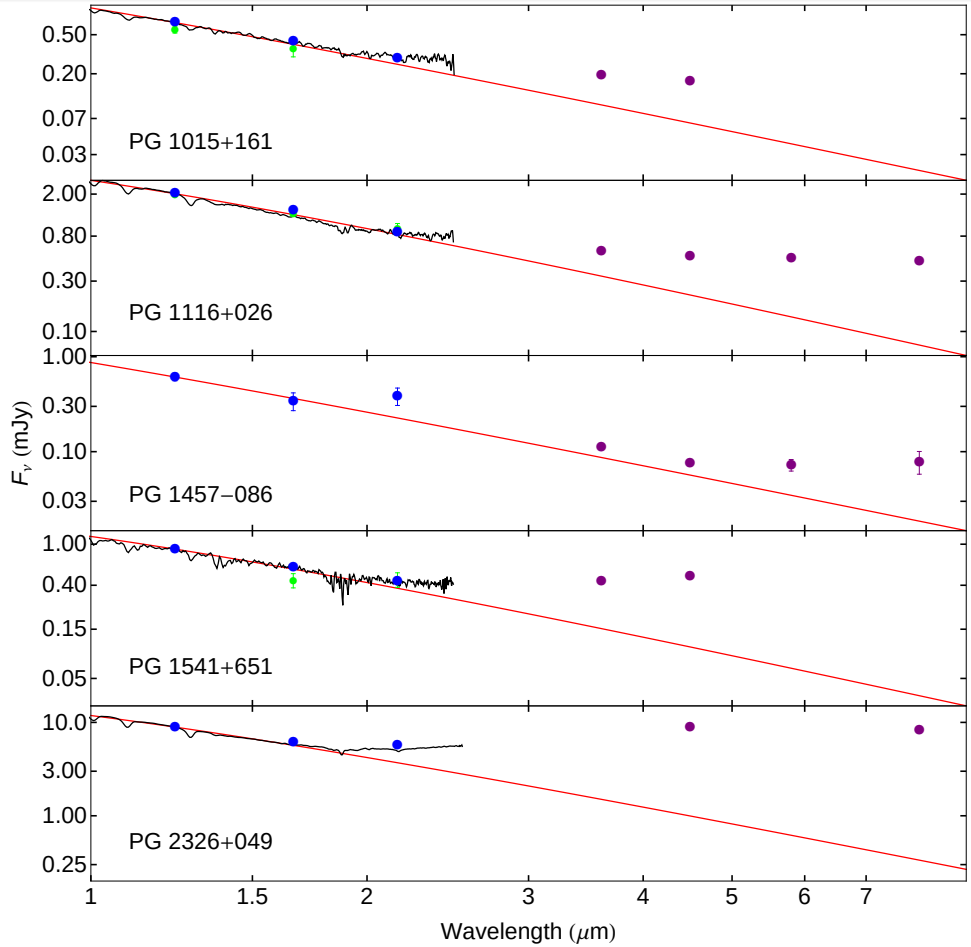

Figure: Five white dwarfs with detections of excess IR radiation

Error Analysis

- Binomial probability distribution function

$$P_n(N,p) = (N+1)\frac{N!}{n!(N-n)!}p^n(1-p)^{N-n}$$

- 68% confidence confidence level (1σ Gaussian)

$$\int_{p_{low}}^{1} P_n(N,p)dp = \int_{0}^{p_{up}} P_n(N,p)dp = 0.84$$

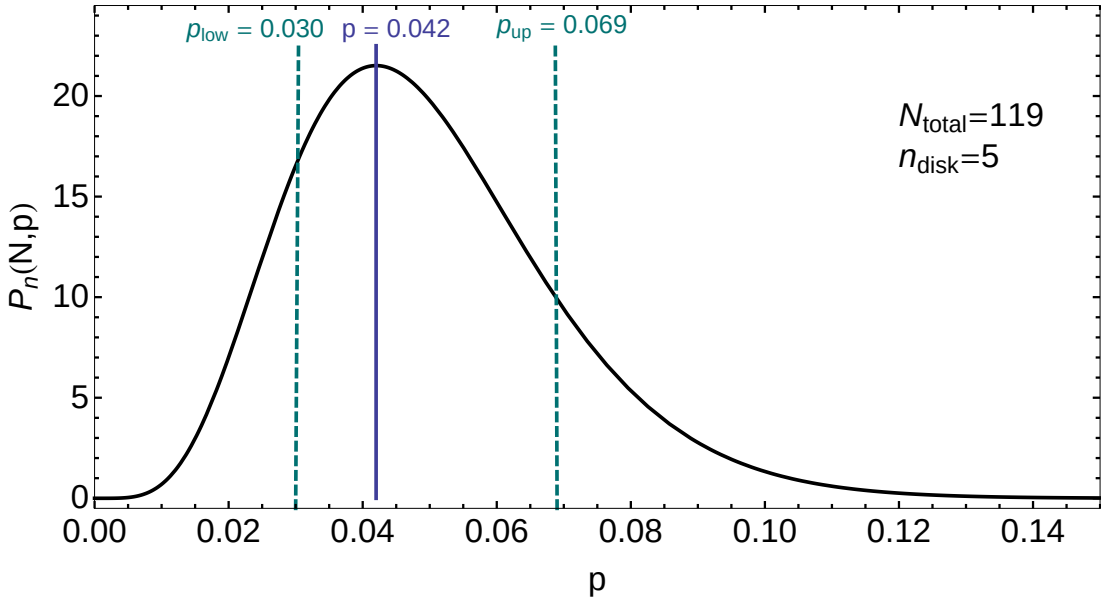

Initial-Final Mass Relation

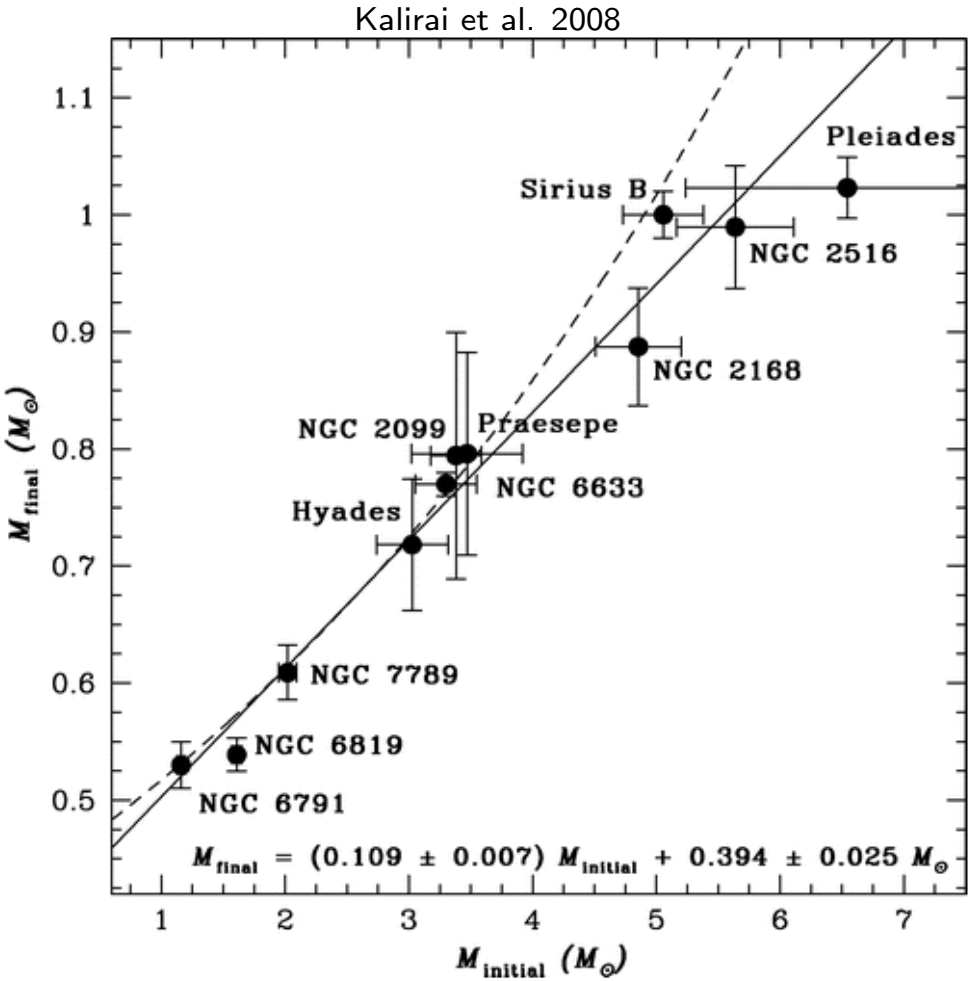

Figure: Initial-final mass relation

- Average MS mass $= 2.3 M_\odot$
- MS mass range $= 1.1 - 7.2 M_\odot$

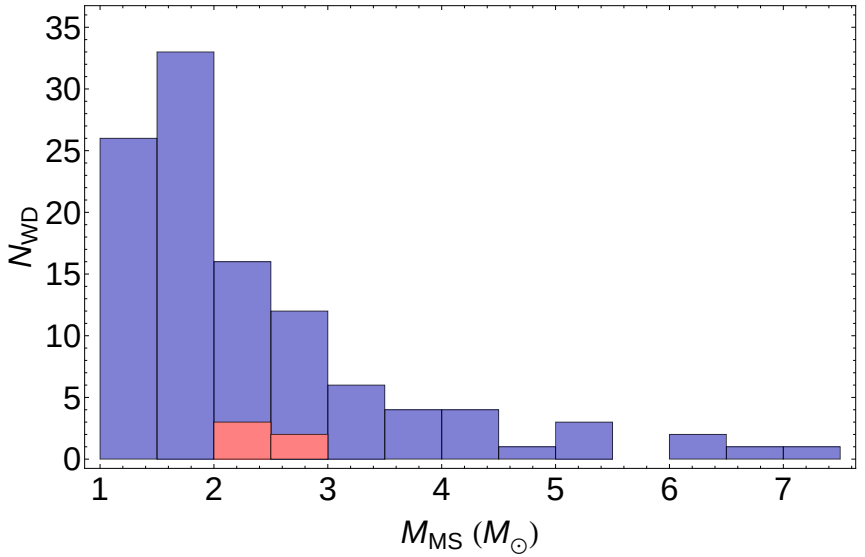

- Frequency of planets around $1 - 7 M_\odot$ MS stars $\geq 4.2^{+2.7}_{-1.2}\%$

Conclusions

1. Frequency of debris disks around WDs $4.2^{+2.7}_{-1.2}\%$
2. Debris disks persist for $4.2^{+2.7}_{-1.2}\%$ WD cooling time
   - Average cooling age $= 340$ Myr
   - Observed WD accretion rate $= 10^{8} - 10^{11}$ g/s
   - Average total mass accreted $= \begin{cases} 0.003 - 3.0\ M_{\rm pluto} \\ 0.0006 - 0.6\ M_{\rm luna} \end{cases}$
3. Frequency of planets around $1 - 7 M_{\odot}$ MS stars $\geq 4.2^{+2.7}_{-1.2}\%$

Menagerie of Disks

John Debes

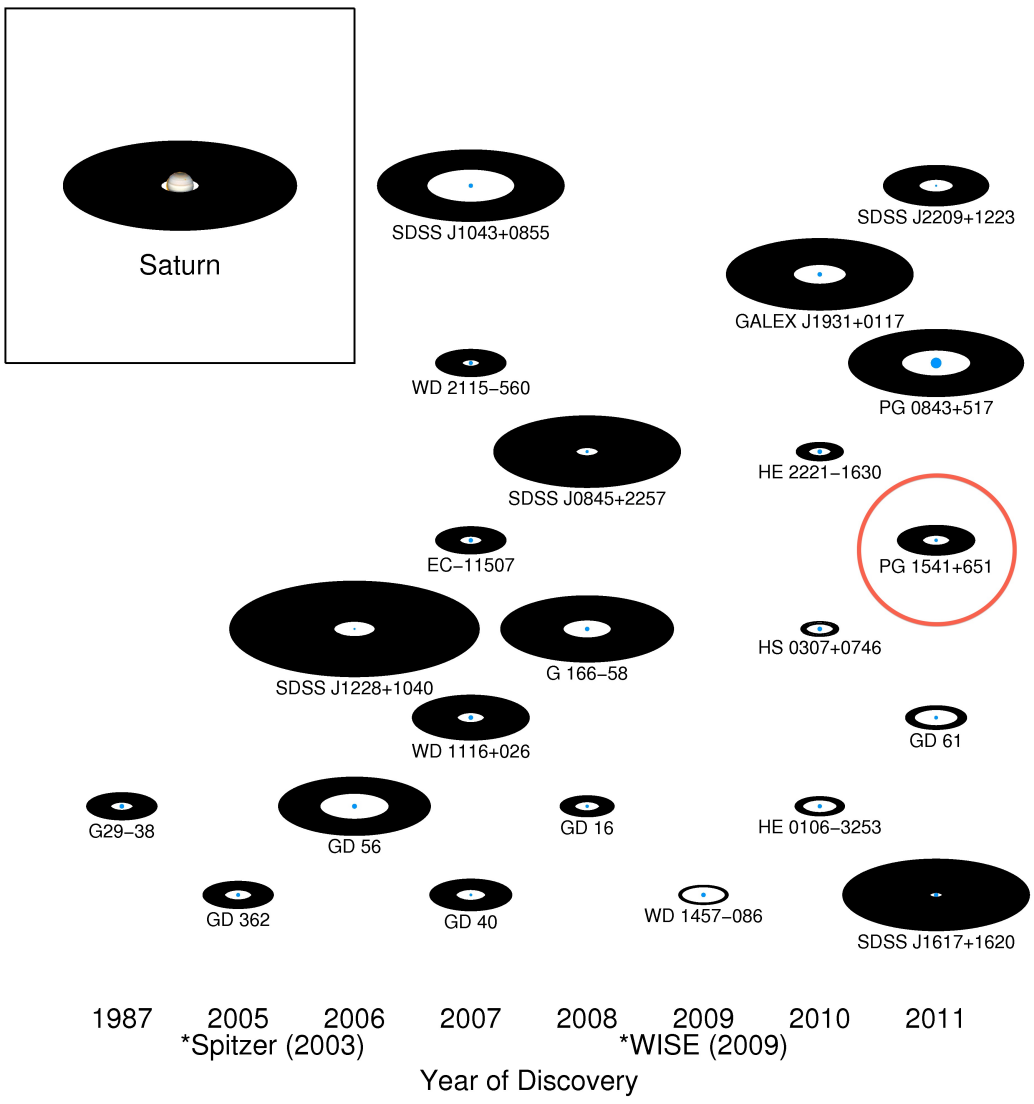

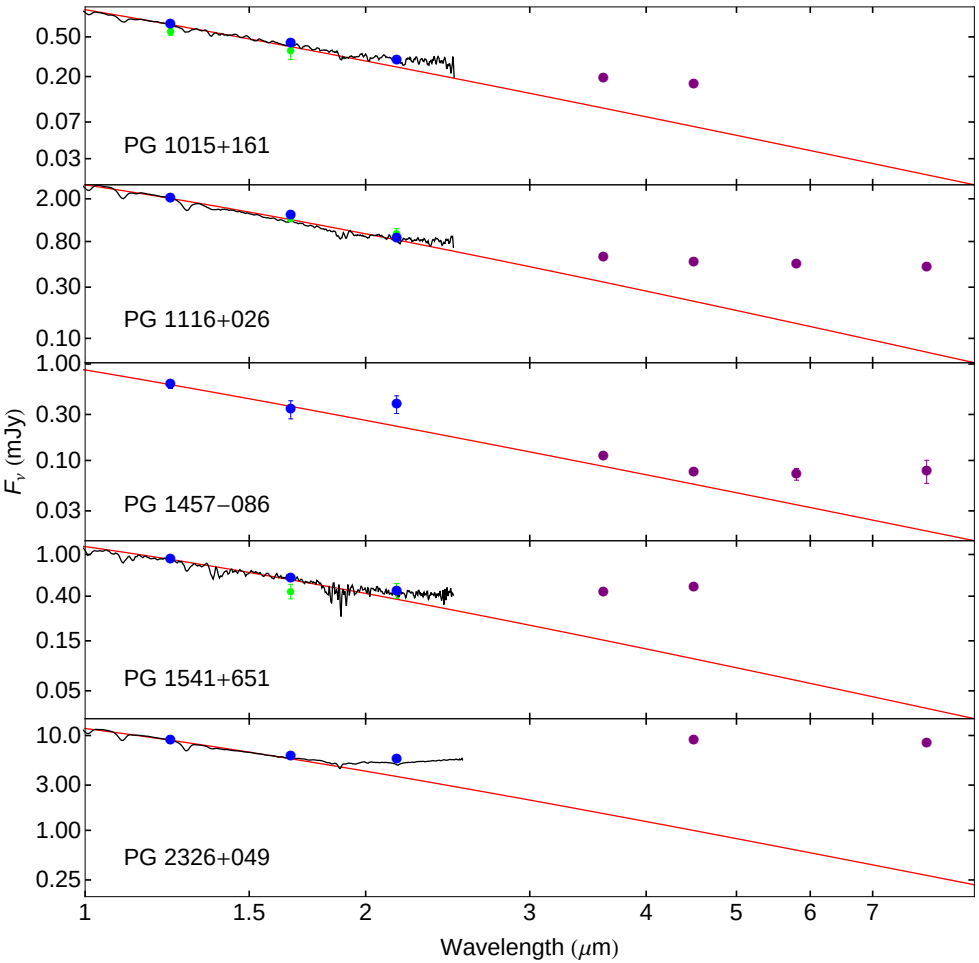
PG 1015+161
PG 1116+026
PG 1457−086
PG 1541+651
PG 2326+049
F_ν (mJy)
Wavelength (μm)

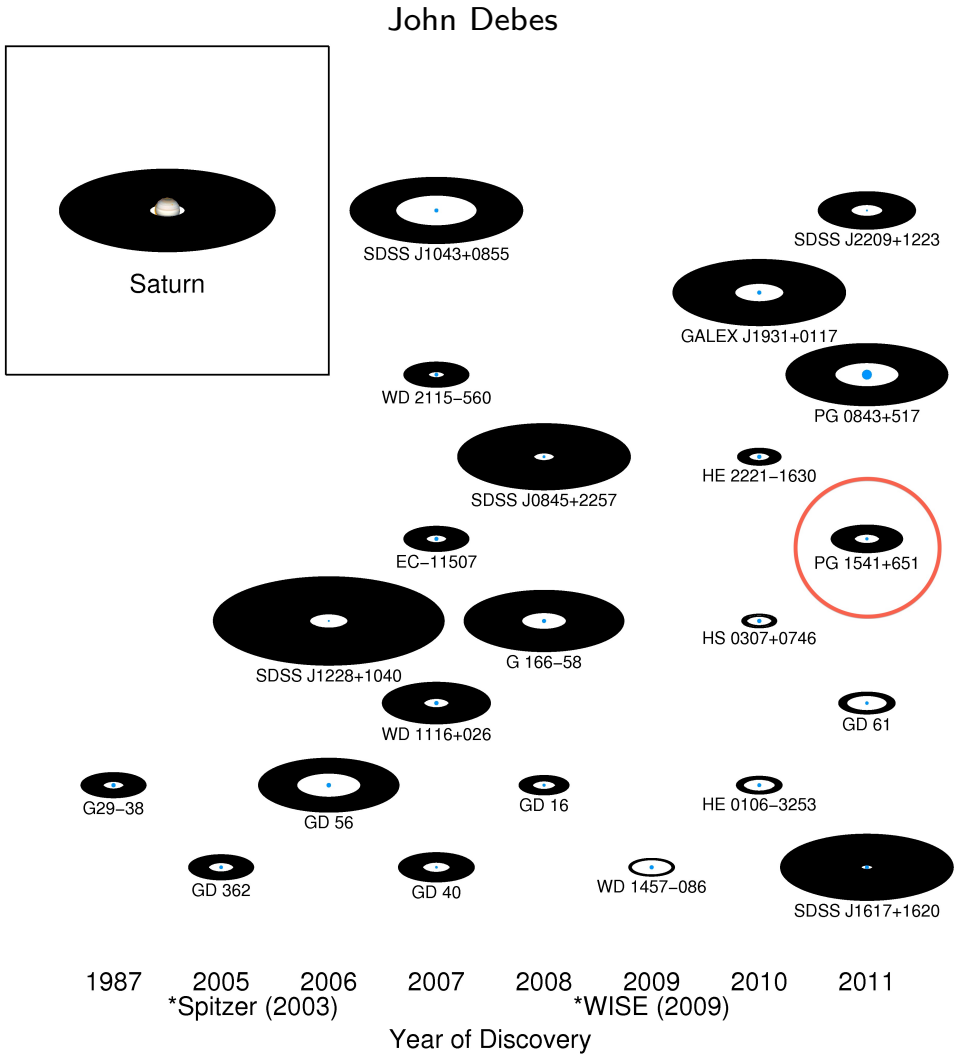
John Debes
Saturn
SDSS J1043+0855
SDSS J2209+1223
GALEX J1931+0117
WD 2115−560
PG 0843+517
SDSS J0845+2257
HE 2221−1630
EC−11507
PG 1541+651
HS 0307+0746
SDSS J1228+1040
G 166−58
WD 1116+026
GD 61
G29−38
GD 56
GD 16
HE 0106−3253
GD 362
GD 40
WD 1457−086
SDSS J1617+1620
1987
2005
2006
2007
2008
2009
2010
2011
*Spitzer (2003)
*WISE (2009)
Year of Discovery

Future Work

- Wide-field Infrared Survey Explorer
- All-sky imaging survey in 3, 5, 12, and 22 μm
- Data released March 2012
- Expand sample

NASA/JPL

Figure: WISE prior to 2009 launch

I would like to thank Dr. Kilic and Adam Patterson for their help on this project.

ESO